

Ferromagnetism of Nuclear Matter in the Relativistic Approach

Tomoyuki Maruyama^{1,2,3} and Toshitaka Tatsumi⁴

¹ *College of Bioresource Sciences, Nihon University, Fujisawa, 252-8510, Japan*

² *RI Beam Science, RIKEN, Wako 351-0198, Japan*

³ *Japan Atomic Energy Research Institute, Tokai, Ibaraki 319-1195*

⁴ *Department of Physics, Kyoto University Kyoto 606-8502, Japan*

Abstract

We study the spin-polarization mechanism in the highly dense nuclear matter with the relativistic mean-field approach. In the relativistic Hartree-Fock framework we find that there are two kinds of spin-spin interaction channels, which are the axial-vector and tensor exchange ones. If each interaction is strong and different sign, the system loses the spherical symmetry and holds the spin-polarization in the high-density region. When the axial-vector interaction is negative enough, the system holds ferromagnetism.

1 Introduction

Recent discovery of "Magnetar" [1], which is a neutron star with super strong magnetic field, seems to revive a big question on the origin of the strong magnetic field. Since there is spread bulk hadronic matter beyond the nuclear density inside neutron stars, it should be interesting to consider its origin in the context of dynamics of hadronic matter; e.g., if the spin-polarization of baryons are realized in nuclear matter, ferromagnetism may occur in neutron stars.

For quark matter, one of the authors (T.T.) has recently indicated a possibility of spin-polarization of quarks interacting with one-gluon-exchange (OGE) interaction [2]; the Fock exchange interaction between quarks has a role to align spins, which is similar to the electron system [3]. Using this result he suggested that super strong magnetic field expected in magnetars may be explained if they are quark stars. There he also found *relativistic effects* give rise to a new mechanism for ferromagnetism, which is never appeared in the nonrelativistic case.

As for the normal nuclear matter Pandharipande et al. [4] have reported no possibility of stable spin-polarization within the non-relativistic framework; magnetic susceptibility never changes its sign within densities relevant for neutron stars.

On the other hand Niembro et al. [5, 6] have suggested a possibility of spin-polarized nuclear matter using the relativistic Hartree-Fock (RHF) approach [7], though spontaneous spin-polarization occurs at too high density. The results in Refs. [5, 6] suggest that the relativistic framework may be more favorite for spin-polarization than the nonrelativistic one. Checking their framework we find some problems about the calculation. First, they implicitly defined the spin-polarization of the system by using the eigenstates of the spin operator $\Sigma_z (= \sigma_z \otimes 1) = \gamma_5 \gamma_0 \gamma^3$ in the rest frame of each particle, and all the particles take the same eigenvalues in the fully polarized state. This may be a direct analogue of the nonrelativistic ferromagnetism. However, the spin operator cannot commute with Hamiltonian in the relativistic theories and thereby we must carefully treat two polarization degrees of freedom for baryons. Actually their choice is not a unique choice; the spin states of all the baryons do not necessarily need to be the eigenstates of the spin operator even in their rest frames. Instead, the spin orientation should depend on the momentum of each particle. Thus we must consider the spin configuration of the spin-polarized state in the phase space.

Secondly, they kept spherical symmetry during the formulation though the spin-polarized system may break it due to the existence of a specific direction (we can assign it as the z axis without loss of generality) along the nonzero magnetization vector in the spin-polarized state. The interaction-energy density has generally the additional momentum dependence besides that

from the propagator in the relativistic theories due to the lower component of the Dirac spinor. Since there should be appeared a characteristic direction in the spin-polarized state, there is another scalar product of momentum and the unit vector along the z axis besides that of momenta in the interaction energy density; the expression of the interaction energy density is no longer rotation-invariant and retains only the rotational symmetry around the z axis. This may in turn suggest a possibility of axially symmetric deformation of the Fermi sphere.

Thirdly, they used in Refs.[5, 6] the σ , ω , ρ and π -meson exchange for the RHF calculation. In reality these interactions should be considered to be the in-medium one, not the bare one, and we do not have any enough information for the two-body interaction which should be used there, especially for the spin-spin interaction channels.

Putting these remarks aside, we know there has been no systematic and sufficient discussions on this topic in the relativistic many-body approach [8], particularly in view of the relativistic effects. For example, the usual calculation, either in the non-relativistic or relativistic framework, has been done under the assumption of spherical symmetry for the mean fields. In this paper we reexamine the spin-polarization of nucleon matter within the RHF approach, focusing on the breaking down of spherical symmetry and importance of the relativistic effects. Since it has been shown in Refs.[2, 5, 6] that the Fock exchange interaction plays a key role in the context of the spin polarization, we must treat this matter within the RHF approach. Then we take some choices of the spin-vectors dependent on the momentum of each particle, and study relations between nuclear properties and these choices.

In the next section we give our formalism, where we clarify what kinds of interactions are effective for the spin-polarization and figure out the role of the spherical symmetry breaking. We also classify the various spin configurations in the relativistic formulation, whereas there is a unique choice in the nonrelativistic theories. Results of numerical calculations are given in Sec. 3. Sec. 4 is devoted to summary and concluding remarks.

2 Formalism

In this section we briefly explain our formulation to describe the spin-polarized system. There should appear a special direction along the spin-polarization; it is defined to be oriented to the positive z -direction. Such a system breaks spherical symmetry while the axial symmetry around the z -axis is preserved.

In the RHF framework the interaction energy density in the isospin saturated system is

generally written as

$$\begin{aligned}
\epsilon_{int} = & \frac{1}{2} \int \frac{d^4p}{(2\pi)^3} \frac{d^4k}{(2\pi)^3} d^4k [\text{Tr}\{iS(p)\} \mathcal{D}_S(p-k) \text{Tr}\{iS(k)\} \\
& + \text{Tr}\{iS(p)\gamma_\mu\} \mathcal{D}_V(p-k) \text{Tr}\{iS(k)\gamma^\mu\} \\
& + \text{Tr}\{iS(p)\gamma_5\} \mathcal{D}_P(p-k) \text{Tr}\{iS(k)\gamma_5\} \\
& + \text{Tr}\{iS(p)\gamma_5\gamma_\mu\} \mathcal{D}_A(p-k) \text{Tr}\{iS(k)\gamma_5\gamma^\mu\} \\
& + \text{Tr}\{iS(p)\sigma_{\mu\nu}\} \mathcal{D}_T(p-k) \text{Tr}\{iS(k)\sigma^{\mu\nu}\}] \quad (1)
\end{aligned}$$

for the one-boson exchange type interaction, assuming no derivative coupling. Here $S(p)$ is the nucleon propagator with momentum p , \mathcal{D}_α ($\alpha = S, V, P, A, T$) is the linear combination of meson-propagators with the nucleon-meson couplings. Note that these interaction terms do not necessarily appear in the original Lagrangian, and that some of them are given by other ones by way of the Fierz transformation. When using the σ - (scalar), ω - (vector) and η - (pseudo-scalar) meson exchanges, for example,

$$\mathcal{D}_S(q) = -\frac{g_\sigma^2}{m_\sigma^2} + \frac{1}{8}g_\sigma^2\Delta_\sigma(q) - \frac{1}{2}g_\omega^2\Delta_\omega(q) + \frac{1}{8}g_\eta^2\Delta_\eta(q) \quad (2)$$

$$\mathcal{D}_V(q) = \frac{g_\omega^2}{m_\omega^2} + \frac{1}{8}g_\sigma^2\Delta_\sigma(q) + \frac{1}{4}g_\omega^2\Delta_\omega(q) - \frac{1}{8}g_\eta^2\Delta_\eta(q), \quad (3)$$

$$\mathcal{D}_P(q) = -\frac{g_\eta^2}{m_\eta^2} + \frac{1}{8}g_\sigma^2\Delta_\sigma(q) + \frac{1}{2}g_\omega^2\Delta_\omega(q) + \frac{1}{8}g_\eta^2\Delta_\eta(q), \quad (4)$$

$$\mathcal{D}_A(q) = \frac{1}{8}g_\sigma^2\Delta_\sigma(q) - \frac{1}{4}g_\omega^2\Delta_\omega(q) + \frac{1}{8}g_\eta^2\Delta_\eta(q), \quad (5)$$

$$\mathcal{D}_T(q) = \frac{1}{8}g_\sigma^2\Delta_\sigma(q) - \frac{1}{8}g_\eta^2\Delta_\eta(q), \quad (6)$$

where g_a ($a=\sigma, \omega$ and η) is the nucleon-meson coupling strength, and Δ_a is the meson-propagator,

$$\Delta_a(q) = \frac{1}{m_a^2 - q^2} \quad (a = \sigma, \omega). \quad (7)$$

The first constant term g_σ^2/m_σ^2 (g_ω^2/m_ω^2) in \mathcal{D}_S (\mathcal{D}_V) indicates the Hartree direct contribution, and other terms are the Fock exchange contributions. Introducing other mesons or vertex form-factors to couplings do not change the form of eq. (1).

In the spin-polarized system, the expectation value of the spin operator Σ_z has a nonvanishing value, and thereby at least the axial-vector (A) and tensor (T) exchange terms survive in eq. (1) as well as the scalar (S) and vector (T) terms. Then the nucleon self-energy must include their contributions, and the ground state breaks parity and spherical symmetries.

In the relativistic mean-field (RMF) approach we usually neglect the momentum dependence of the propagator because the nucleon-nucleon interaction can be effectively treated as the zero-range one in low energy phenomena as far as the typical energy and/or momentum scale is much

less than the meson mass. Actually only very small momentum dependence has appeared in the full RHF calculation [7, 9]. Here, we take the zero-range approximation for two nucleon interaction which can be described as follows:

$$\mathcal{D}_\alpha = \frac{\tilde{C}_\alpha}{2M^2} \quad (\alpha = S, V, P, A, T). \quad (8)$$

Even with this approximation the RHF calculation is still complicated because there appear the axial-vector and tensor mean fields. These parity violation terms largely mix the positive-energy and negative-energy states in the single particle wave-function. Thus completely self-consistent calculations become very complicated and must be done very carefully as for the vacuum polarization. Furthermore we do not have sufficient information of all channels of the in-medium interaction between nucleons, especially in the axial-vector and tensor channels. Thus we will not get any clear conclusion in spite of very tough calculations by solving the RHF equation self-consistently. Instead of solving the exact self-consistent RHF equation, we take a variational approach in the RHF framework.

The two degrees of freedom of the spin polarization for each nucleon is denoted by $\zeta = 1$ and $\zeta = -1$, which we call spin-up and -down, respectively. Then we take the nucleon propagator with four-momentum p in the following form;

$$S(p, \zeta) = S_F(p, \zeta) + S_D(p, \zeta) \quad (9)$$

with the propagators of a vacuum piece (S_F) and a density-dependent piece (S_D),

$$S_F(p, \zeta) = \frac{\{\gamma_\mu p^{*\mu} + M^*\}}{p^{*2} - M^{*2}} \frac{\{1 + \gamma_5 \not{a}(p^*, \zeta)\}}{2}, \quad (10)$$

$$S_D(p, \zeta) = \{\gamma_\mu p^{*\mu} + M^*\} \frac{\{1 + \gamma_5 \not{a}(p^*, \zeta)\}}{2} \frac{i\pi}{E_p^*} n(\mathbf{p}, \zeta) \delta(p_0 - \varepsilon_p), \quad (11)$$

where $p^{*\mu} \equiv p^\mu - U^\mu$, $M^* = M - U_s$ and $E_p^* = \sqrt{\mathbf{p}^2 + M^{*2}}$. In these equations U_s and U_μ are the scalar and vector mean fields, and ε_p is the single particle energy of the nucleon with momentum \mathbf{p} , $\varepsilon_p = E_p^* + U_0$. $a(p^*, \zeta)$ is the spin-vector of the nucleon with momentum p which satisfies the following conditions:

$$a_\mu a^\mu = -1, \quad a_\mu p^{*\mu} = 0. \quad (12)$$

In the following we only keep the density-dependent piece S_D with the momentum distribution function $n(\mathbf{p}, \zeta)$ to be determined, for which we assume the axial symmetry along the spin-polarization. Note that this form of the propagator is the same as the one when the nucleon self-energy includes only scalar U_s and vector U_μ mean fields, which are independent of the

nucleon's spin. Moreover, we can easily see that the expectation value of the pseudoscalar operator automatically vanishes,

$$\text{Tr}\{iS(p)\gamma_5\} = 0. \quad (13)$$

So the pseudoscalar (P) term in Eq. (1) vanishes in this case.

Then the total energy density ϵ_T is separated into two parts: the spin-independent part ϵ_{SID} and the spin-dependent part ϵ_{SD} as

$$\epsilon_T = \epsilon_{SID} + \epsilon_{SD}. \quad (14)$$

The axial-vector and tensor exchange channels contribute to the spin-dependent part ϵ_{SD} while the kinetic energy and contributions from the scalar and vector channels are involved in the spin-independent one ϵ_{SID} .

Under the zero-range approximation the spin-independent part of the Fock contribution can be incorporated into the Hartree one. Then it is possible to redefine the two-body scalar interaction by taking into account the Fock terms, which corresponds to the usual relativistic Hartree (RH) approximation. Thus we can write the scalar mean-field by the expectation value of the σ field $\langle\sigma\rangle$ as

$$U_s = g_\sigma \langle\sigma\rangle, \quad (15)$$

and calculate the effective mass M^* with the usual RH approximation. The expectation value $\langle\sigma\rangle$ is given by the equation,

$$\frac{\partial}{\partial\langle\sigma\rangle}\tilde{U}[\langle\sigma\rangle] = g_\sigma \rho_s = g_\sigma \sum_{\zeta} \rho_s(\zeta), \quad (16)$$

where the scalar density is defined as

$$\rho_s(\zeta) = \int \frac{d^3p}{(2\pi)^3} n(\mathbf{p}; \zeta) \frac{M^*}{E_p^*}, \quad (17)$$

and $\tilde{U}[\sigma]$ is the self-energy potential of the sigma-field, whose expression is given in Ref. [10, 11].

$$\tilde{U}[\sigma] = \frac{\frac{1}{2}m_\sigma^2\sigma^2 + \frac{1}{3}B_\sigma\sigma^3 + \frac{1}{4}C_\sigma\sigma^4}{1 + \frac{1}{2}A_\sigma\sigma^2}. \quad (18)$$

In the RH approximation, furthermore, the spatial components of the vector mean-field are vanished, and the time component is given as

$$U_0 = g_\omega \rho_B = g_\omega \sum_{\zeta} \rho_B(\zeta), \quad (19)$$

where $\rho_B(\zeta)$ is the baryon density contributed from nucleon with the spin suffix ζ as

$$\rho_B(\zeta) = 2 \int \frac{d^3p}{(2\pi)^3} n(\mathbf{p}; \zeta). \quad (20)$$

Under this formulation the spin-independent part of the energy density ϵ_{SID} becomes

$$\epsilon_{SID} = 2 \sum_{\zeta} \int \frac{d^3 p}{(2\pi)^3} n(\mathbf{p}; \zeta) E_p^* + \tilde{U}[\sigma] + \frac{g_{\omega}^2}{2m_{\omega}^2} \left[\sum_{\zeta} \rho_B(\zeta) \right]^2, \quad (21)$$

while the spin-dependent energy density ϵ_{SD} is calculated to be,

$$\epsilon_{SD} = \frac{\tilde{C}_A}{2M^2} \rho_A^2 + \frac{\tilde{C}_T}{2M^2} \rho_T^2 \quad (22)$$

with the axial-vector and tensor densities,

$$\rho_A = \int \frac{d^4 p}{(2\pi)^4} Tr\{S_D(p) \gamma_5 \gamma^3\} = \rho_B \langle \Sigma_z \rangle = \sum_{\zeta} \int \frac{d^3 p}{(2\pi)^3} n(\mathbf{p}; \zeta) \frac{M^*}{E_p^*} a_z \quad (23)$$

$$\rho_T = \int \frac{d^4 p}{(2\pi)^4} Tr\{S_D(p) \sigma_{12}\} = \rho_B \langle \beta \Sigma_z \rangle = \sum_{\zeta} \int \frac{d^3 p}{(2\pi)^3} n(\mathbf{p}; \zeta) \left\{ a_z - \frac{p_z}{E_p^*} a_0 \right\} \quad (24)$$

Other components of the axial-vector and tensor densities are vanished because of the axial symmetry of the momentum distribution. Note that the axial-vector and the tensor interactions, even though they are not necessarily included in the original Lagrangian, may arise from the Fock exchange interactions by way of the Fierz transformation, as is seen in Eqs. (5) and (6). In this sense we can say that the Fock exchange interaction is essential for the system to be ferromagnetic [2, 5, 6].

In order to figure out the properties of the spin-polarized matter, we solve RH equation (16) and calculate the energy-density by fixing the baryon density ρ_B and the spin-polarization parameter x_s defined by

$$x_s \equiv (\rho_{\uparrow} - \rho_{\downarrow}) / \rho_B. \quad (25)$$

where $\rho_{\uparrow} = \rho_B(\zeta = 1)$ and $\rho_{\downarrow} = \rho_B(\zeta = -1)$. (For convenience the spin-up and spin-down states are indicated by the symbols \uparrow and \downarrow , respectively.)

In our approach the wave-function is not an exact solution of the Dirac equation in the mean-fields. So we need to specify the spin configuration in the system by choosing a spin-vector a_{μ} . Once it is fixed, the momentum distribution of the single-particle state should be also determined accordingly. The best way to this end is to choose the configuration to optimize the total energy density ϵ_T , while it may be rather complicated. Instead, we examine here the following three choices by physical considerations.

The total spin-polarization is directed to the positive direction of the z -axis; here we define a unit vector $\boldsymbol{\zeta}_m = (0, 0, \zeta)$. Usually the spin-vector a_{μ} is chosen as $(0, \boldsymbol{\zeta}_m)$ at the rest frame of the nucleon, we should call this choice as Choice-1(Ch1). This choice may be a natural extension from the nonrelativistic ferromagnetism and has been also taken in the context of

ferromagnetism of quark matter [2]. Then the spin-vector with momentum \mathbf{p} becomes

$$\mathbf{a} = \left[\boldsymbol{\zeta}_m + \frac{(\boldsymbol{\zeta}_m \cdot \mathbf{p})\mathbf{p}}{M^*(E_p^* + M^*)} \right], \quad a^0 = \frac{\boldsymbol{\zeta}_m \cdot \mathbf{p}}{M^*}, \quad (26)$$

by way of the Lorentz transformation. In this choice ρ_A and ρ_T can be written as

$$\rho_A = \frac{1}{3} \sum_{\zeta} \zeta \{ 2\rho_s(\zeta) + \rho_B(\zeta) \}, \quad (27)$$

$$\rho_T = \frac{1}{3} \sum_{\zeta} \zeta \{ \rho_s(\zeta) + 2\rho_B(\zeta) \}. \quad (28)$$

Then the interaction-energy density can be written only in terms of the scalar $\rho_s(\zeta)$ and vector densities $\rho_B(\zeta)$ of nucleons with the spin ζ , and the expression still holds spherical symmetry. In the high-density limit, as mentioned before, the scalar density ρ_s approaches to a finite value in the RMF approach [8], and its contribution becomes negligible, so that we can see that $\rho_A^2 < \rho_T^2$ in the limit $\rho_B \rightarrow \infty$. Hence the spin-polarization occurs when $\tilde{C}_A + 4\tilde{C}_T < 0$. The above choice does not necessarily lead to the state with the spin-alignment, and the total spin per nucleon converges to one-third ($\langle \Sigma_z/A \rangle = \rho_A/\rho_B \rightarrow x_s/3$) in the infinite density limit; magnetization is not so large even if all the nucleon spins align.

Here we consider another choice, Choice-2(Ch2) for the vector a_μ to give the maximum for $|a_z|$ within our framework. In this new choice the spin-vector becomes

$$a_0 = \frac{E_p^*(\boldsymbol{\zeta}_m \cdot \mathbf{p})}{M^* \sqrt{(\boldsymbol{\zeta}_m \cdot \mathbf{p})^2 + M^{*2}}}, \quad (29)$$

$$\mathbf{a} = \frac{M^{*2}\boldsymbol{\zeta}_m + (\boldsymbol{\zeta}_m \cdot \mathbf{p})\mathbf{p}}{M^* \sqrt{(\boldsymbol{\zeta}_m \cdot \mathbf{p})^2 + M^{*2}}} \quad (30)$$

Substituting the above form into eqs.(23) and (24), we get

$$\rho_A = 2 \sum_{\zeta} \zeta \int \frac{d^3p}{(2\pi)^3} n(\mathbf{p}; \zeta) \frac{\sqrt{p_z^2 + M^{*2}}}{E_p^*} \quad (31)$$

$$\rho_T = 2 \sum_{\zeta} \zeta \int \frac{d^3p}{(2\pi)^3} n(\mathbf{p}; \zeta) \frac{M^*}{\sqrt{p_z^2 + M^{*2}}} \quad (32)$$

When $\rho_B \rightarrow \infty$, ρ_T converges to a finite value, and ρ_A is proportional to the baryon density ρ_B . If the momentum-distribution $n(\mathbf{p}; \zeta)$ is taken as usual Fermi-distribution, the total spin per nucleon converges

$$\langle \Sigma_z/A \rangle = \rho_A/\rho_B \rightarrow x_s/2. \quad (33)$$

Hence we can expect a ferromagnetic phase as long as $\tilde{C}_A < 0$. We shall see that this choice is the most appropriate for ferromagnetism.

As another choice, Choice-3(Ch3), we take the vector a_μ to give the maximum of the expectation value $\langle \beta \Sigma_z / A \rangle = \rho_T / \rho_B$, which is reduced to the same value as that of the spin operator in the nonrelativistic limit. In this case the spin-vector becomes

$$a_0 = \frac{E_p^*}{M^* \sqrt{\mathbf{p}_T^2 + M^{*2}}} \zeta, \quad (34)$$

$$\mathbf{a} = \frac{\sqrt{\mathbf{p}_T^2 + M^{*2}}}{M^*} \zeta \mathbf{m}, \quad (35)$$

with

$$\mathbf{p}_T = \mathbf{p} - \zeta \mathbf{m} (\zeta \mathbf{m} \cdot \mathbf{p}). \quad (36)$$

Then the axial-vector and tensor densities can be written as

$$\rho_A = 2 \sum_{\zeta} \zeta \int \frac{d^3 p}{(2\pi)^3} n(\mathbf{p}; \zeta) \frac{M^*}{\sqrt{\mathbf{p}_T^2 + M^{*2}}} \quad (37)$$

$$\rho_T = 2 \sum_a \zeta \int \frac{d^3 p}{(2\pi)^3} n(\mathbf{p}; \zeta) \frac{\sqrt{\mathbf{p}_T^2 + M^{*2}}}{E_p^*}. \quad (38)$$

In this choice ρ_A and ρ_T show the opposite behaviors in the infinite density limit; ρ_A converges to a finite value, and ρ_T is proportional to the baryon density ρ_B . Hence the system becomes spin-polarized state when $\tilde{C}_T < 0$. However, the expectation value of the spin operator Σ_z has a nonvanishing value and becomes

$$\langle \Sigma_z / A \rangle = \rho_A / \rho_B \rightarrow 0, \quad (39)$$

which means that the system is not ferromagnetic in a usual sense.

Since the spin-dependent energy ϵ_{SD} depends on the coupling strengths, \tilde{C}_A and \tilde{C}_T , we have to carefully determine which choice is most appropriate. In the low density region $\rho_A \approx \rho_T \approx x_s \rho_B$, the spin-saturated system should be stable and then the two coupling constants \tilde{C}_A and \tilde{C}_T must satisfy the following relation

$$\tilde{C}_A + \tilde{C}_T > 0. \quad (40)$$

If $\tilde{C}_A \geq 0$ and $\tilde{C}_T \geq 0$, the spin-saturated system must be stable in all the density region, and spherical symmetry is always held. Otherwise the analysis at the infinite density limit show us that system becomes spin-polarized if $\tilde{C}_A < 0 < \tilde{C}_T$ (Ch2) or $\tilde{C}_T < 0 < \tilde{C}_A$ (Ch3) holds. Even in Ch1 the spin-polarization can occur if $\tilde{C}_A + 4\tilde{C}_T < 0$, but this condition expects large negative \tilde{C}_T and the spin-vector of a nucleon prefers Ch3 than Ch1.

Furthermore we should note that the above expressions of eq.(31) and eq.(32) do not preserve spherical symmetry. The relativistic effects automatically give rise to the spherical symmetry

breaking. From this fact we can naturally expect that the momentum distribution $n(\mathbf{p}; \zeta)$ is allowed to be distorted while keeping the axial-symmetry. In order to estimate the effects of distortion of the momentum distribution, we introduce the quadrupole-distorted distribution function $n(\mathbf{p})$ as

$$n(\mathbf{p}; \zeta) = n_0(e^{\lambda(\zeta)} p_x, e^{\lambda(\zeta)} p_y, e^{-2\lambda(\zeta)} p_z; \zeta), \quad (41)$$

where $n_0(\mathbf{p}; \zeta) = \theta(p_F(\zeta) - |\mathbf{p}|)$ with the Fermi-momentum p_F . The parameter $\lambda(\zeta)$ is determined to give the energy minimum of the spin-polarized system.

As mentioned in the previous section, the two contributions from the axial-vector and tensor channels are not considered in the original interactions; instead they are derived by the Fierz transformation from the Fock exchange interactions in other channels. Using several parameters given in previous works, however, we get various spin-properties even at the normal nuclear density. For example the parameter-sets of HF-I in Ref. [7], within the σ - and ω - meson exchanges, gives us $\tilde{C}_A = -8.55$ and $\tilde{C}_T = 30.2$, and the parameter-sets with π -, σ -, ρ - and π (PS)- meson exchanges in Ref. [6], gives us $\tilde{C}_A = 3210$ and $\tilde{C}_T = -3200$. The latter extraordinary value comes from the pion-exchange ($M^2 g_\pi^2 / m_\pi^2 = 8200$), which never allow the zero-range interaction approximation. Thus the values of two coupling strengths, \tilde{C}_A and \tilde{C}_T , are still very ambiguous, and they cannot be individually determined at present both in theoretical and experimental ways. Instead of using parameters given in previous papers, we investigate the spin-polarization of nuclear matter by varying the values of \tilde{C}_A and \tilde{C}_T in this paper.

As discussed above, we have a possibility to get ferromagnetic matter only in the case of $\tilde{C}_A < 0 < \tilde{C}_T$, where Ch2 for the spin-vector must be most appropriate. Hence we study the spin-properties only in this case except in some figures where properties are also calculated with Ch1 for comparison. We shall see that ferromagnetism can occur due to the spherical symmetry breaking in the relativistic framework, by concrete numerical calculations in the next section.

3 Results and Discussions

In this section we make concrete calculations as for the spin-polarized nuclear matter and discuss their consequences. We calculate physical quantities concerning the magnetic properties only for the isospin symmetric matter and make comparison with neutron matter in the final place. In the actual procedure, first, we evaluate the sigma-field with eq.(16) by fixing baryon density ρ_B and the spin-polarization parameter $x_s \equiv (\rho_\uparrow - \rho_\downarrow) / \rho_B$; namely we solve the RH equation. Secondly, we substitute the result into eqs. (31) and (32), and obtain the spin-dependent energy ϵ_{SD} in eq.(22). Repeating these processes by varying $\lambda_\uparrow \equiv \lambda(\zeta = 1)$ and

$\lambda_{\downarrow} \equiv \lambda(\zeta = -1)$, we search the energy minimum.

The parameter-sets PM1 ($M^*/M = 0.7$) and PM4 ($M^*/M = 0.55$) are used for the RH calculation; the definite values of the parameters are given in Table 1. In Fig. 1 we show the density-dependence of the total energy per nucleon (E_T/A) and the effective mass normalized by the bare mass (M^*/M). The values of the coupling strengths in the axial-vector and tensor channels must be consistent with the spin-properties at normal nuclear density such as the spin-symmetry energy. We here define the spin-symmetry energy, inversely proportional to the magnetic susceptibility by

$$\varepsilon_{sp-sym} = \frac{\partial^2 E_T/A}{\partial \langle \Sigma_z/A \rangle^2} \Big|_{x_s=0}. \quad (42)$$

In this work we take its value as $\varepsilon_{sp-sym} = 25(\text{MeV})$, while it is not clearly determined from experimental information¹, and we use three kinds of the parameter-set: $\tilde{C}_A = 0$ (SD1), $\tilde{C}_A = -50$ (SD2) and $\tilde{C}_A = -100$ (SD3). Here we restrict ourselves to the cases with $\tilde{C}_A < 0$, since matter would be ferromagnetic only in this case. The detailed values of parameters are given in Table 2.

In Fig. 2 we show the density-dependence of the spin-symmetry energies ε_{sp-sym} with PM1 (a) and PM4 (b). If this value becomes negative, the spin-saturated system becomes unstable and the spin-polarized one is favored. The long-dashed, dashed and solid lines indicate results for SD1, SD2 and SD3, respectively. For all the parameter-sets the spin-symmetry energy increases in the low density region as baryon density becomes larger. While the spin-symmetry energy monotonously increases in the case of $\tilde{C}_A = 0$ (SD1), it decreases and becomes minus above a critical density ρ_c for the cases of negative \tilde{C}_A (SD2 and SD3): $\rho_c/\rho_0 = 8.74$ for SD2 and $\rho_c/\rho_0 = 4.28$ for SD3. Note that the spin-symmetry energies are smaller in high-density region in PM4 than in PM1, The parameter-set PM4 gives rise to a smaller effective mass than PM1, and the decrease of the effective mass enlarges ε_{sp-sym} if the coupling strengths \tilde{C}_A and \tilde{C}_T are fixed. Since we fix the spin-symmetry energy at the saturation density, however, the coupling constant \tilde{C}_T becomes small for the small effective mass; then contributions from the axial-vector channel get larger in PM4.

In the infinite density limit the effective mass M^* goes to zero (Fig. 1b) and the scalar-density ρ_s converge to the finite value in the RMF theory. Thus ρ_A and ρ_T must have density-dependence similar to ρ_B and ρ_S , respectively; namely, when $\rho_B \rightarrow \infty$, ρ_T converges to a finite value and ρ_A is proportional to the baryon density ρ_B . In this limit, then, only the kinetic

¹The spin-symmetry energy is written as $\varepsilon_{sp-sym} = (p_F^2/6m^*)(1 + G_0)$ with the nonrelativistic effective mass m^* and the Landau parameter G_0 . This value is given as 26 MeV by a realistic nuclear matter calculation [12] and 10 – 60 MeV by the Skyrme interaction [13, 14, 15].

energy and the axial vector exchange channels contribute to the spin-symmetry energy ε_{sp-sym} . Since $\langle \Sigma_z/A \rangle \sim x_s$ around the spin-saturated matter, the contribution from the kinetic energy is proportional to $\rho_B^{2/3}$ in the low density limit and to $\rho_B^{1/3}$ in the high-density limit. On the other hand the contribution from the axial-vector exchange channels is proportional to $\tilde{C}_A \rho_B$ in the high-density limit; this behavior should be the same as the density-dependence of the (isospin-) symmetry energy. From this fact we can easily see that, if $\tilde{C}_A < 0$, the spin-symmetry energy becomes negative and the spin-polarization spontaneously occurs above a certain critical density.

In Fig. 3 some quantities are shown as functions of the spin-polarization parameter x_s at $\rho_B = \rho_0$ (dotted line), $3\rho_0$ (dashed line), $5\rho_0$ (solid line) and $6\rho_0$ (chain-dotted line). We give the energy difference from that at the spin-saturated matter $\Delta E_T/A = (E_T(x_s) - E_T(x_s = 0))/A$ (a), M^*/M (b), the total spin per nucleon $\langle \Sigma_z/A \rangle = \rho_A/\rho_B$ and the deformation parameters λ_\uparrow and λ_\downarrow .

In Fig. 3a it can be seen that above $\rho_B > 5\rho_0$ the value of the spin-polarization parameter at the energy-minimum moves from $x_s = 0$ to a finite value, whose value becomes larger as baryon density increases. There is a single local energy-minimum at the fixed density. Thus the phase transition from normal matter to the spin-polarized one is of the second order.² To occur the first order phase-transition we need an interaction energy which is negative and proportional to at least $\langle \Sigma_z/A \rangle^4$. The axial-vector term in the interaction energy has the role to give rise to a spin-polarization, and it is exactly proportional to $\langle \Sigma_z/A \rangle^2$. On the contrary we can see in Fig. 3b that the effective mass is very slightly varied with the spin-polarization parameter, and thereby we can conclude that the scalar interaction does not largely contribute the spin-polarization.

In Fig. 3c we can see that at high density the value of $\langle \Sigma_z/A \rangle = \rho_A/\rho_B$ becomes slightly smaller than that in the fully polarized system. From eq. (31) we can easily understand this behavior by considering that the small effective mass reduces the expectation value of the nucleon spin due to the relativistic effect ($M^*/E_p^* < 1$).

In Fig. 3d it can be seen that at high density the momentum distribution gets the prolate deformation for spin-up nucleons and the oblate deformation for spin-down nucleons; these deformations enhance ρ_A (31) and decrease ρ_T (32).

In Fig. 4 we show the equation of states for the fully spin-polarized nuclear matter ($x_s = 1$), the density-dependence of $\Delta E_T/A$ (a), $\langle \Sigma_z/A \rangle$ (b) and the deformation parameters for the

²It should be interesting to compare this result with the one in quark matter [2].

spin-up nucleons $\lambda(\zeta = 1)$ (c), with the three spin-dependent parameter-sets (SD1–3). As increasing \tilde{C}_A the deformation becomes larger, keeping rather large value of $\langle \Sigma_z/A \rangle$, which in turn implies that the phase transition more easily occurs.

When $\tilde{C}_A < 0$, the axial-vector exchange interaction plays a role to decrease the total energy by enlarging $\langle \Sigma_z/A \rangle$ with the variation of x_s and $\lambda_{\uparrow(\downarrow)}$. On the other hand these variations enhances the kinetic and scalar exchange energies; the latter is not seen to be so effective because the effective mass slightly changes from the spin-symmetric value (see Fig. 3b).

In order to examine effects of the spherical symmetry breaking, in Fig. 5, we show the spin-symmetry energy ε_{sp-sym} using three kinds of choices (Ch1, Ch2-S, Ch2-Q). Ch2-S and -Q are the two versions of Ch2: the spin-vector of Ch2 (eq.(30)) with the spherical (Ch2-S) and the quadrupole-deformed momentum distribution (Ch2-Q).

In Ch1 the spin-symmetry energy always monotonously increases when density becomes larger; the reason has been given in the previous section. In Ch2-S the qualitative behavior is almost the same as that for Ch2-Q though the value of ε_{sp-sym} and the critical density are always larger than those for Ch2-Q. When $\tilde{C}_A < 0$, the spherical symmetry breaking for the spin-vector makes a critical effect for the spin-polarization. In addition such effects from the choice of the spin-vector are enhanced by the deformation of the momentum distribution (Fig. 4c). Hence the axial-vector correlation between two nucleons rather easily gives rise to the ferromagnetic state through the spherical symmetry breaking.

In Fig. 6 we show the density dependence of $\langle \Sigma_z/A \rangle = \rho_A/\rho_B$ (a) and $\langle \beta \Sigma_z/A \rangle = \rho_T/\rho_B$ (b) at $x_s = 1$ using Ch1 (dotted line), Ch2-S (dashed line) and Ch2-Q (solid line), and the quadrupole deformation parameter for spin-up nucleons λ_{\uparrow} using Ch2-Q (c). The parameter-sets PM1 and SD1 are used in this calculation.

With increase of density, the difference among three choices becomes prominent: the total spin per nucleon $\langle \Sigma_z/A \rangle$ decreases for Ch1 and Ch2-S, while it does not become so small for Ch2-Q (see Fig. 7a). This behavior can be understood from the analysis at the infinite density limit. In this limit, as mentioned before, the effective mass approaches to the zero value, and thereby $\langle \Sigma_z/A \rangle \rightarrow x_s/3$ for Ch1 (see eq.(27)) and $\langle \Sigma_z/A \rangle \rightarrow x_s/2$ for Ch2-S (see eq.(31)); in any choice of the spin-vector the total spin, in the relativistic framework, becomes much less than that in the non-relativistic one. On the other hand the choice Ch2-Q gives

$$\langle \Sigma_z/A \rangle \rightarrow \frac{1 + x_s}{2(1 + e^{-6\lambda_{\uparrow}})} - \frac{1 - x_s}{2(1 + e^{-6\lambda_{\downarrow}})}. \quad (43)$$

In the limit of $\lambda_{\uparrow} \rightarrow \infty$ and $\lambda_{\downarrow} \rightarrow -\infty$, $\langle \Sigma_z/A \rangle \rightarrow (1 + x_s)/2$; of course this limit makes infinite kinetic energy so that the $\lambda_{\uparrow(\downarrow)}$ finally has a moderate value. Thus the deformation of

the momentum distribution plays a significant role to give a large value of the total spin. The prolate deformation of the momentum distribution recovers the reduction of the total spin in the high-density region.

Furthermore it can be seen in Fig. 6b that $\langle \beta\Sigma_z/A \rangle$ decreases for Ch2-S and Ch2-Q with increase of density, while its value does not becomes small. As discussed in the previous section, $\langle \beta\Sigma_z/A \rangle \rightarrow 2x_s/3$ for Ch1 and $\langle \beta\Sigma_z/A \rangle \rightarrow 0$ for Ch2-S and Ch2-Q in the infinite density limit ($M^* \rightarrow 0$). In addition we see that the value of $\langle \beta\Sigma_z/A \rangle$ in Ch2-Q is always smaller than that in Ch2-S, and we know here again that the deformation of the momentum distribution plays a important role through the reduction of $\langle \beta\Sigma_z/A \rangle$.

From these results we confirm that the choice of the spin-vector is very important for the spin-polarization, and that we have to use Ch2 instead of Ch1 if $\tilde{C}_A < 0$. In the Refs. [5, 6] the coupling \tilde{C}_A becomes positive, though the interaction is not zero-range, and then Ch2 may not be appropriate. Then there remain Ch1 and Ch3; they used Ch1.

As made before, the analysis at the infinite density limit must be useful to examine it qualitatively. In this limit the spin-dependent part of the energy density becomes

$$\epsilon_{SD} \approx \frac{1}{18}(\tilde{C}_A + 4\tilde{C}_T)\rho_B^2 x_s^2 \quad (inCh1) \quad (44)$$

$$\epsilon_{SD} \approx \frac{\pi^2}{32}\tilde{C}_T\rho_B^2 x_s^2 \quad (inCh3) \quad (45)$$

where we assume that the momentum-distribution holds the spherical symmetry. To get smaller energy in Ch1 than in Ch3,

$$\frac{1}{9}(\tilde{C}_A + 4\tilde{C}_T) < \frac{\pi^2}{16}\tilde{C}_T \quad (46)$$

and this equation leads to a condition that $\tilde{C}_A < 1.55\tilde{C}_T$, which is inconsistent with the condition $\tilde{C}_T < 0 < \tilde{C}_A$. In addition, the deformation of the momentum distribution further reduces ϵ_{SD} in Ch3.

If $\tilde{C}_T < 0 < \tilde{C}_A$, then, Ch3 must become reasonable. We can suppose that the qualitative behavior must be similar to that of Ch2-Q. As the density becomes larger, namely, ρ_A converges to a finite value, and ρ_T increases proportionally to the density, and then the phase-transition occurs at a certain critical density. In this case the momentum distribution is deformed with the oblate shape for the spin-up ($\lambda_\uparrow < 0$) and with the prolate for the spin-down ($\lambda_\downarrow > 0$). From this consideration we can expect that the total energy should be smaller in Ch3 than that in Ch1 at any density if $\tilde{C}_T < 0 < \tilde{C}_A$.

From the above results we can see the particular role of the spherical symmetry breaking through the choice of the spin-vector and the distortion of the momentum distribution. They

becomes very important in high-density region due to decreasing of the nucleon effective mass.

As mentioned in Sec. I the spontaneous spin-polarization is expected to occur in the high-density region inside neutron stars, though we have studied the magnetic properties only at the symmetric nuclear matter. We did because we would like to clarify the discussion by avoiding extending the formulation to include the isovector channel. We expect to determine the spin-spin interactions in the relativistic framework from some experimental information in future. However we may have some meaning to compare results at neutron matter with that at symmetric nuclear matter within the formulation given in this paper. In Fig. 7 we show the density dependence of the spin-symmetry energy with PM1 and SD(1-3) for Ch2. The thick and thin lines indicate results at neutron matter and at symmetric nuclear matter, respectively. We cannot see any significant difference between them except that ε_{sp-sym} at neutron matter is a little larger than that at symmetric nuclear matter.

4 Summary and Concluding remarks

In this paper we have examined a possible mechanism of the spin-polarization of nucleons and discussed magnetic properties of the system. In the relativistic framework there are two kinds of spin-spin interaction channels, the axial-vector and tensor ones, which are reduced to the same interaction channels in the nonrelativistic framework. If the interaction energies from two channels have opposite signs, there is a second-order phase transition to a spin-polarized state. Though the effects from two channels are counterbalanced with each other around the normal density, the channel with the negative sign becomes dominant, suppresses the spin-symmetry energy with increase of density and induces a phase-transition in a certain critical density ρ_c . In this mechanism the spherical symmetry breaking through the spin vector and the momentum distribution plays a significant role; the spherical symmetric calculation (Ch1) cannot describe such a phase-transition sufficiently.

These qualitative findings can be easily derived from the analysis at the infinite density limit, which is equivalent to the ultra relativistic limit in the present framework. Actual numerical calculations confirm them, so that the consideration in this limit is very useful to predict qualitative behaviors of matter at high density.

If the tensor channel is largely negative, the total nucleon spin becomes large while the total spin converges to zero at the infinite density limit. Thus such system cannot make strong ferromagnetism even at high density, Inside actual neutron stars the density is not infinite, and we has not known how large ferromagnetism is necessary to explain magnetars. Then we cannot

deny this possibility though we omit it at the present calculations. We should keep it in mind for future.

In this work we represent the strength of these channels with the couplings \tilde{C}_A and \tilde{C}_T by using the zero-range approximation, which makes the Fock exchange interaction local. Then we find that, if $\tilde{C}_A < -100$, the phase-transition occurs in the reasonable density $\rho_B \leq 5\rho_0$, which can be realized inside neutron stars. However, the main purpose of this paper is to reveal the characteristic features of the relativistic ferromagnetism of nuclear matter within the RHF framework. If we want to get a realistic conclusion about the critical density, we need to determine two couplings \tilde{C}_A and \tilde{C}_T individually from the experimental information, while experiments can at present give only nuclear spin properties in low density region around and/or below the normal density. Furthermore, we need the isovector interactions when we consider neutron-star matter.

Two approximations have been introduced in this work. One is that we have applied a variational approach, avoiding the complete self-consistent calculation. If we can do it, some points are improved; the single particle energies become different between the spin-up and -down states, which should in turn determine the modification of the Fermi sea. Because of the variational principle, anyway, these improvements must reduce the total energy in the spin-polarized system. Then the phase transition may occur in the lower density and/or with the smaller couplings of \tilde{C}_A than those in the present calculations.

The other is that we have used the zero-range approximation for the meson propagators and discarded the finite-range effects in the nucleon interactions; the zero-range approximation is equivalent to neglect the momentum-dependence of the self-energies and should be reasonable, at least, at low densities s.t. $m_a \gg p_F$. As for the spin-independent parts it has been reported that the momentum-dependence of the self-energy has a role to reduce the total energy per nucleon (E_T/A) in the high-density region [10, 16] and to suppress largely the Fermi velocity [17], particularly in the low density region. However these effects does not affect the nuclear equation of state at zero temperature. As for the spin-dependent parts the situation must be similar.

These approximations used in our calculations must never spoil our qualitative findings of the relativistic ferromagnetism.

We do not clearly know what phase actually appears inside neutron stars. A quark matter [2] is one possibility and the hyperonic matter is also possible. In the latter case we need to take into account the interaction between hyperon and nucleon and that between hyperons.

We compare here our results with the previous one given by one of the authors (T.T.) for quark matter [2]. It has been shown that ferromagnetism of quark matter may occur at low-density region and it should be the first-order phase transition; all the quark spins suddenly align at the critical density and there is no partially polarized state. The most important difference from nuclear matter is that quarks interact with each other through only the vector interaction by gluons and there is no direct interaction due to color neutrality of quark matter. Moreover there is no tensor channel and the gluon propagator corresponds to the zero-mass limit of Δ_ω . As a result $\mathcal{D}_A(q)$ given in Eq. (5) is always negative and $\mathcal{D}_T(q) \equiv 0$, which is most favorite situation for the system to be ferromagnetic. In this case the momentum dependence of the propagator becomes essential and the phase transition is of the first order due to this effect; if we replace the propagator by some constant, we shall see that phase transition becomes of the second order and there is a partially polarized state as is seen in this paper.

Our findings of the momentum dependence of the spin orientation and possible deformation of the Fermi sea have not been taken into account in ref.[2]. It may be interesting to see these effects in the context of ferromagnetism of quark liquid [18].

ACKNOWLEDGEMENTS

This work was supported in part by the Japanese Grant-in-Aid for Scientific Research Fund of the Ministry of Education, Science, Sports and Culture (11640272).

References

- [1] C. Kouveliotou et al., Nature **393** (1998) 235.
K. Hurley et al., Astrophys. J. **510** (1999) L111.
- [2] T. Tatsumi, Phys. Lett. **B**, in press; hep-ph/9910470(KUNS-1611);
nucl-th/0002014(KUNS-1636); astro-ph/0004062(KUNS-1656).
- [3] F. Bloch, Z. Phys. **57** (1929) 545.
- [4] V.R. Pandharipande, V.K. Garde and J.K. Srivastava, Phys. Lett. **B38** (1972) 485.
- [5] R. Niembro, S. Marcos, M.L. Quelle and J. Navarro, Phys. Lett. **B249** (1990) 373.
- [6] S. Marcos, R. Niembro and M.L. Quelle Phys. Lett. **B271** (1991) 277.
- [7] C. J. Horowitz and B. D. Serot, Nucl. Phys. **A399** (1983) 529.

- [8] B.D. Serot and J. D. Walecka, The relativistic Nuclear Many Body Problem. In J. W. Negele and E. Vogt, editors, *Adv.Nucl.Phys.***Vol.16**, page 1, Plenum Press, 1986, and reference therein.
- [9] K. Soutome, T. Maruyama, K. Saito, Nucl. Phys. **507** (1990) 731.
- [10] T. Maruyama, B. Blättel, W. Cassing, A. Lang, U. Mosel, K. Weber, Phys. Lett **B297** (1992) 228;
T. Maruyama, W. Cassing, U. Mosel, S. Teis and K. Weber, Nucl. Phys **A552** (1994) 571.
- [11] T. Maruyama, H. Fujii, T. Muto and T. Tatsumi, Phys. Lett. **B337** (1994) 19;
H. Fujii, T. Maruyama, T. Muto and T. Tatsumi, Nucl. Phys. **A597** (1996) 645.
- [12] H. Müther, Prog. Prat. Nucl. Phys. **14** (1984) 123.
- [13] E.Chabanat et al., Nucl. Phys. **A627** (1997) 710.
- [14] T. Maruyama, T.-S. Saito and T. Tsukamoto, Prog. Theo. Phys. Vol.**82** (1989) 1009.
- [15] J. Navarro, E.S. Hernandez, and D. Vautherin, hep-ph/901311.
- [16] K. Weber, B. Blättel, W. Cassing, H.-C. Dönges, V. Koch, A. Lang and U. Mosel, Nucl. Phys. **A539** (1992) 713.
- [17] T. Maruyama and S. Chiba, Phys. Rev. **C61**, 037301-1 (2000).
- [18] S. Ushida and T. Tatsumi, in preparation.

Figure Captions

- Fig. 1 Density-dependence of the total energy per nucleon (a), and the ratio of the effective masses to the bare masses for nucleon (b). The solid and dashed lines indicate the results for PM1 and PM4, respectively.
- Fig. 2 Density-dependence of the spin-symmetry energies (ε_{sp-sym}) with PM1 (a) and PM4 (b). The long-dashed, dashed and solid lines indicate results for $\tilde{C}_A = 0$ (SD1), $= -50$ (SD2) and $= -100$ (SD3), respectively.
- Fig. 3 Energy difference between the spin-polarized and saturated systems (a), the effective mass M^* normalize by the bare nucleon mass M (b) the total spin per nucleon $\langle \Sigma_z/A \rangle$ (c) and the deformation parameter λ (d) versus the spin-polarization parameter $(\rho_\uparrow - \rho_\downarrow)/\rho_B$. The dotted, dashed, solid and chain-dotted line indicate results at $\rho_B = \rho_0$, $\rho_B = 3\rho_0$, $\rho_B = 5\rho_0$ and $\rho_B = 6\rho_0$, respectively. In the third column (c) the thick and thin lines indicate ones for the spin-up and spin-down, respectively.
- Fig. 4 The density-dependence of $\Delta E_T/A$ (a), $\langle \Sigma_z/A \rangle$ (b) and the deformation parameters for the spin-up nucleons $\lambda(\zeta = 1)$ (c) with SD1 (dotted line), SD2 (dashed line) and SD3 (solid line). in the fully spin-polarized nuclear matter ($x_s = 1$).
- Fig. 5 Density-dependence of the spin-symmetry energies (ε_{sp-sym}) with PM1 calculated with the method Ch1 (a), Ch2-S (b) and Ch2-Q (c) (seeing text). The meaning of the lines are shown in Fig. 2.
- Fig. 6 The density-dependence of $\langle \sigma_z/A \rangle$ (a) $\langle \beta\sigma_z/A \rangle$ (b) and the deformation parameters for the spin-up nucleons $\lambda(\zeta = 1)$ with SD1 (dotted line), SD2 (dashed line) and SD3 (solid line) in the fully spin-polarized nuclear matter ($x_s = 1$). For the spin-independent parts the parameter-sets of PM1 are used.
- Fig. 7 Density-dependence of the spin-symmetry energies (ε_{sp-sym}) with PM1. The long-dashed, dashed and solid lines indicate results for $\tilde{C}_A = 0$ (SD1), $= -50$ (SD2) and $= -100$ (SD3), respectively. The thick and thin lines indicate results at the neutron matter and at nuclear matter, respectively.

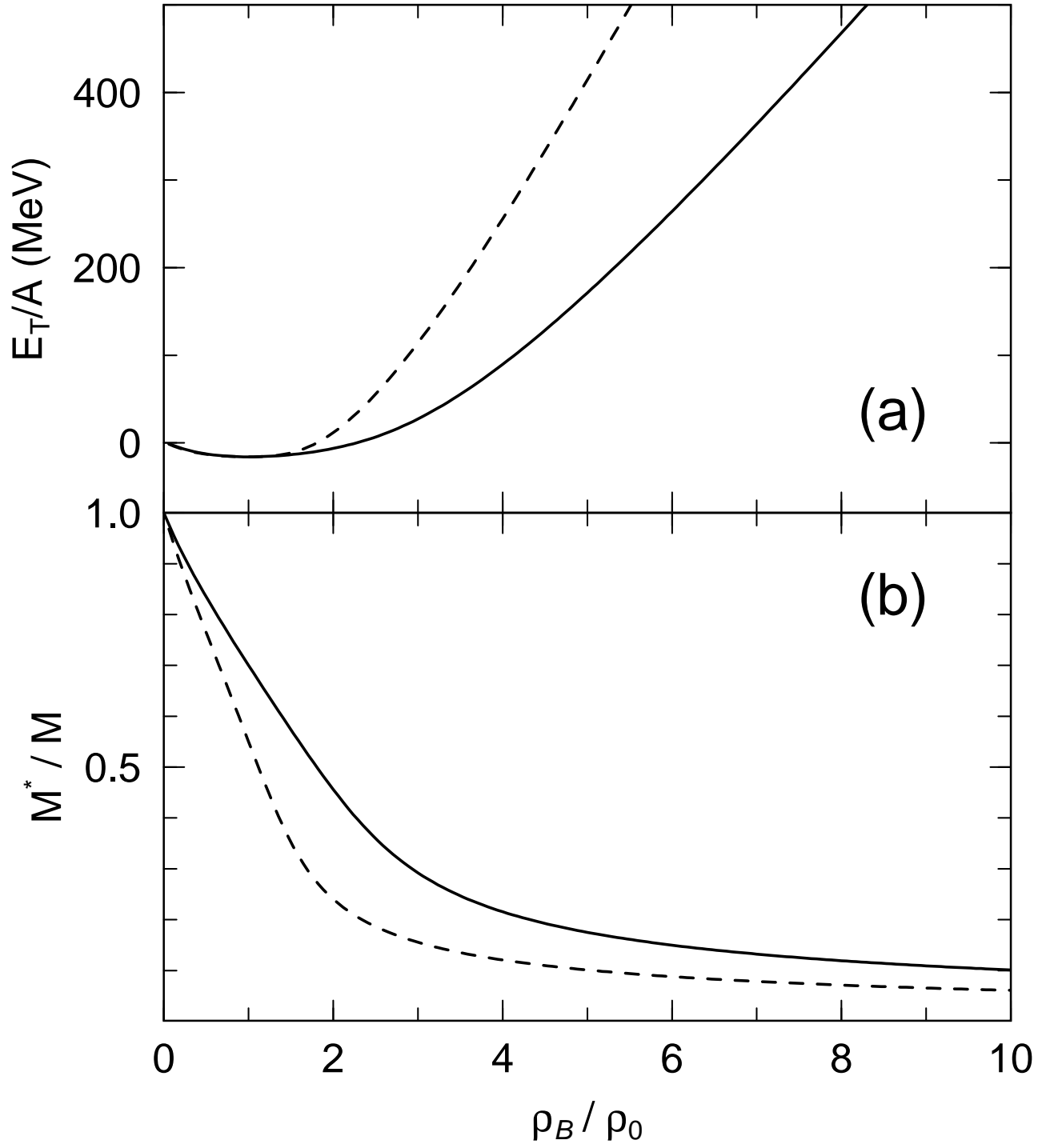
	g_σ	g_ω	B_σ	A_σ
PM1	9.408	9.993	23.52	5.651
PM4	11.05	12.64	18.89	7.158

Table 1: Parameter sets for the RH calculation in this paper. In all cases have used $m_\sigma = 550$ MeV, $m_\omega = 783$ MeV and $C_\sigma = 0$.

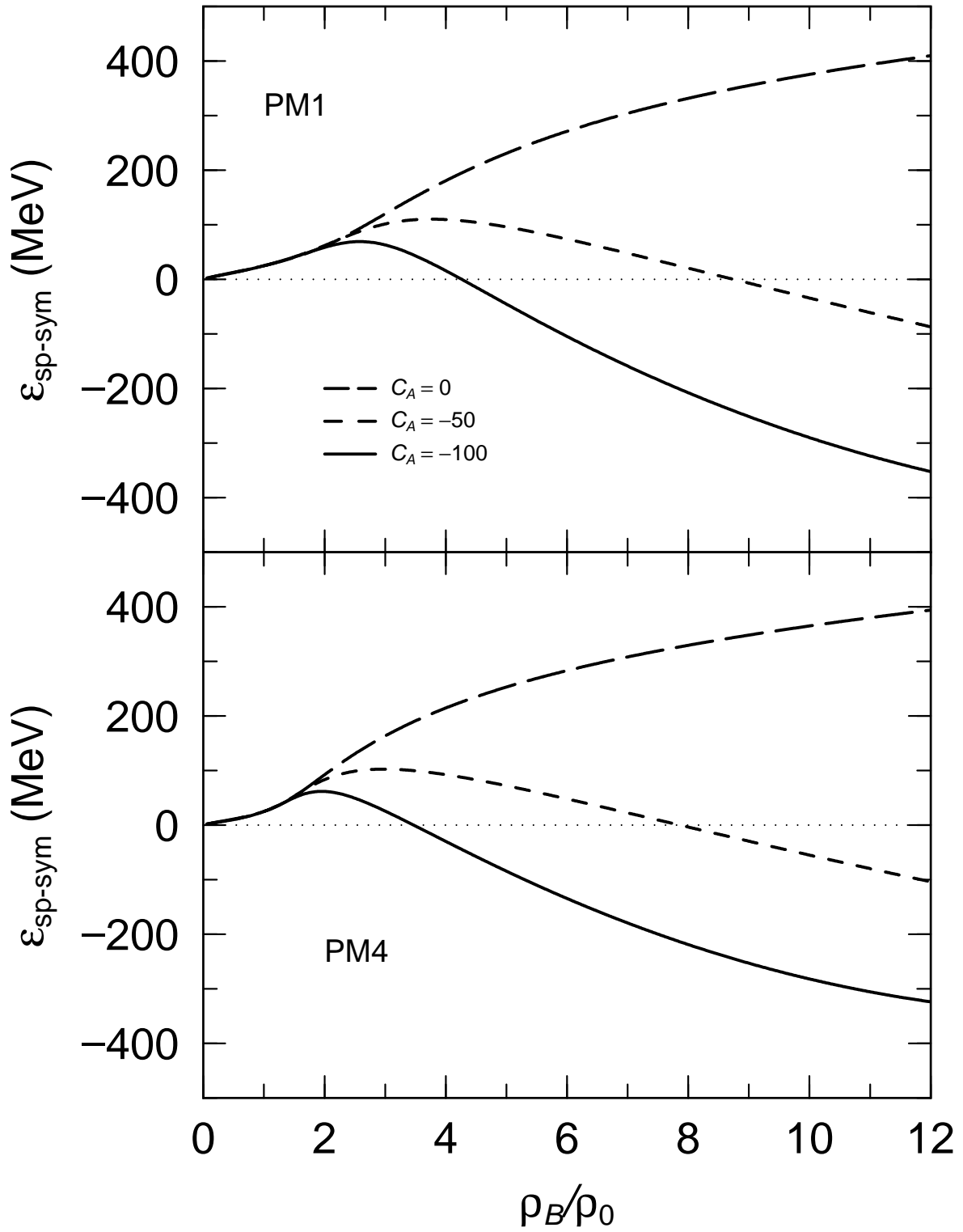
	PM1		PM4	
	\tilde{C}_A	\tilde{C}_T	\tilde{C}_A	\tilde{C}_T
SD1	0	9.993	0	1.1365
SD2	-50	56.10	-50	48.32
SD3	-100	104.5	-50	96.27

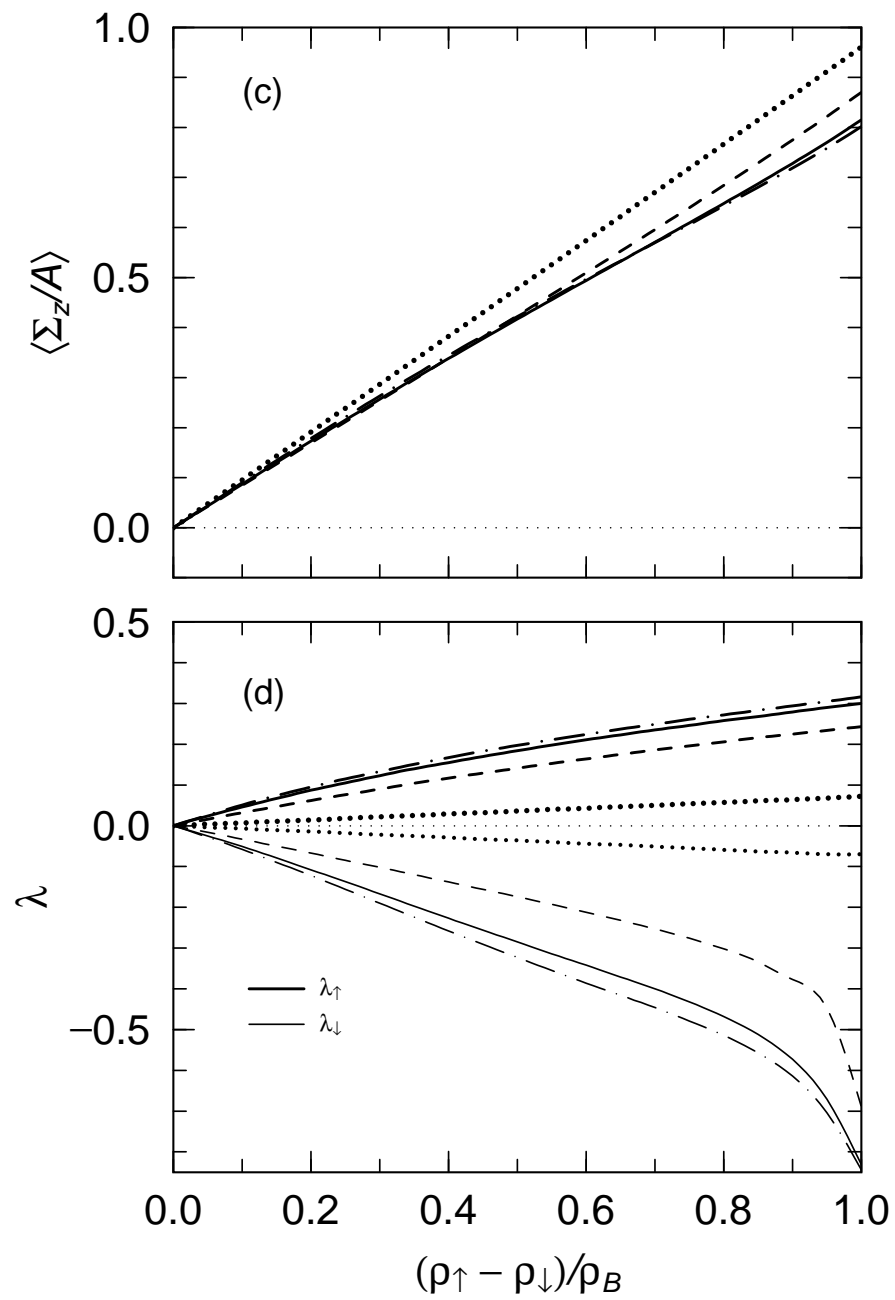
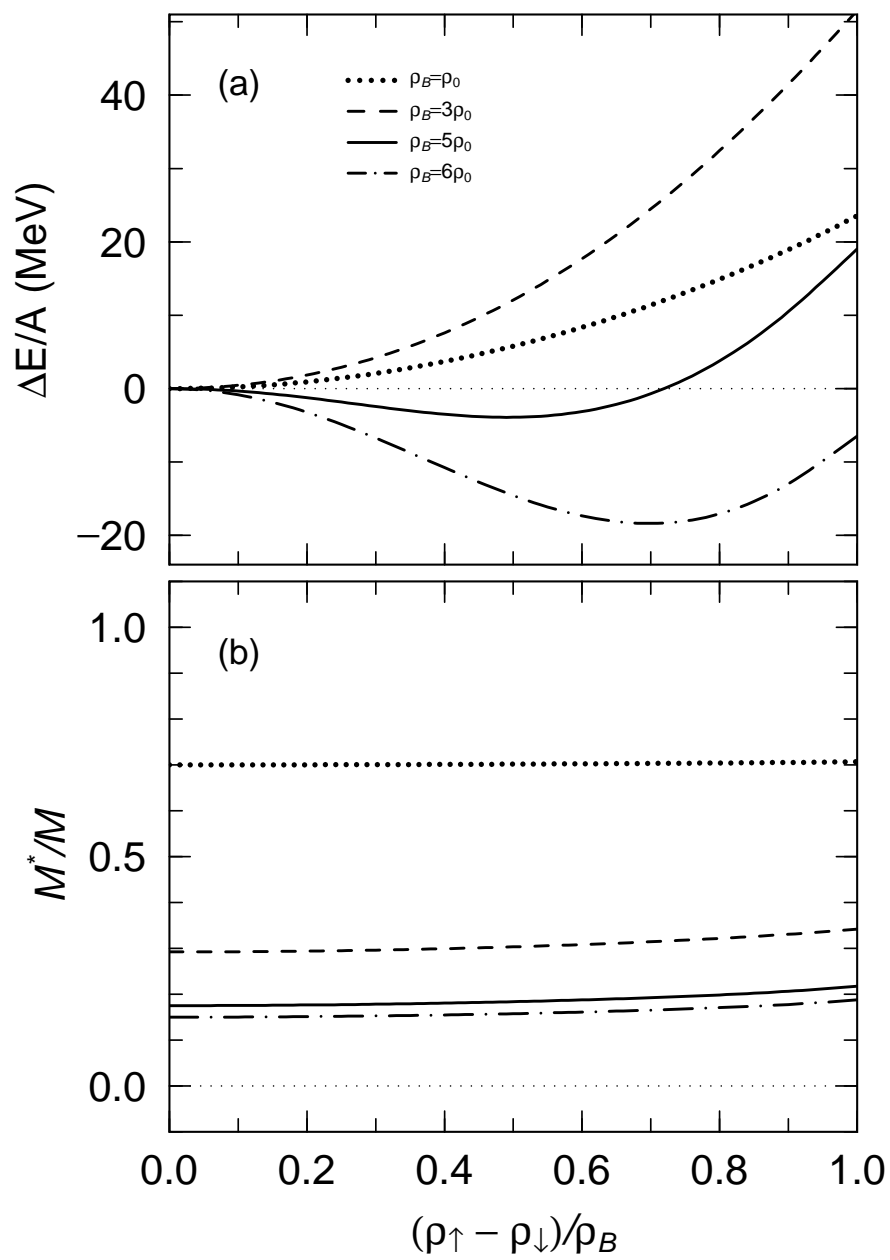
Table 2: Parameter sets for the spin-dependent interactions in this paper.

EQUATION OF STATE

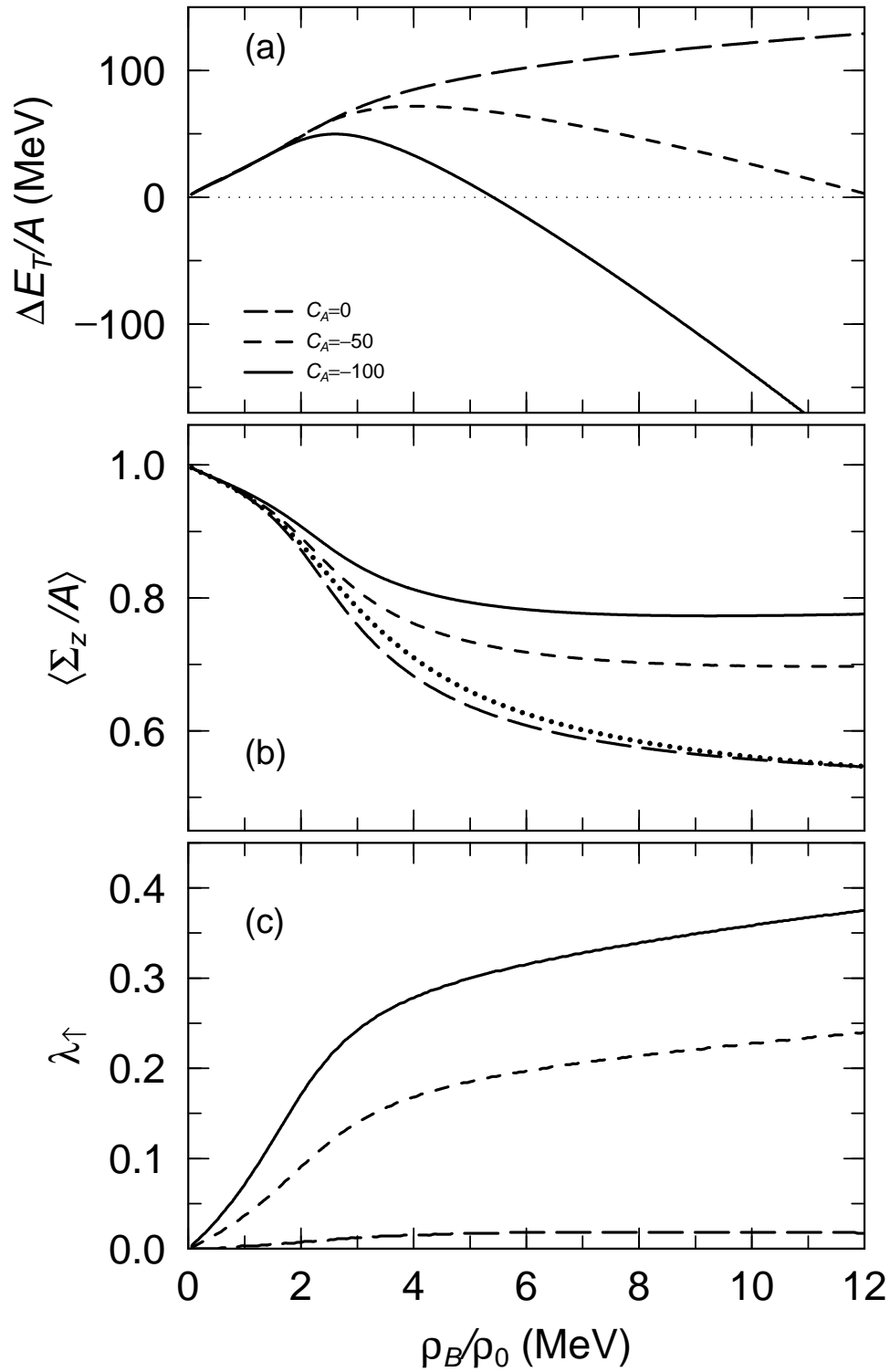


SPIN-SYMMETRY ENERGY

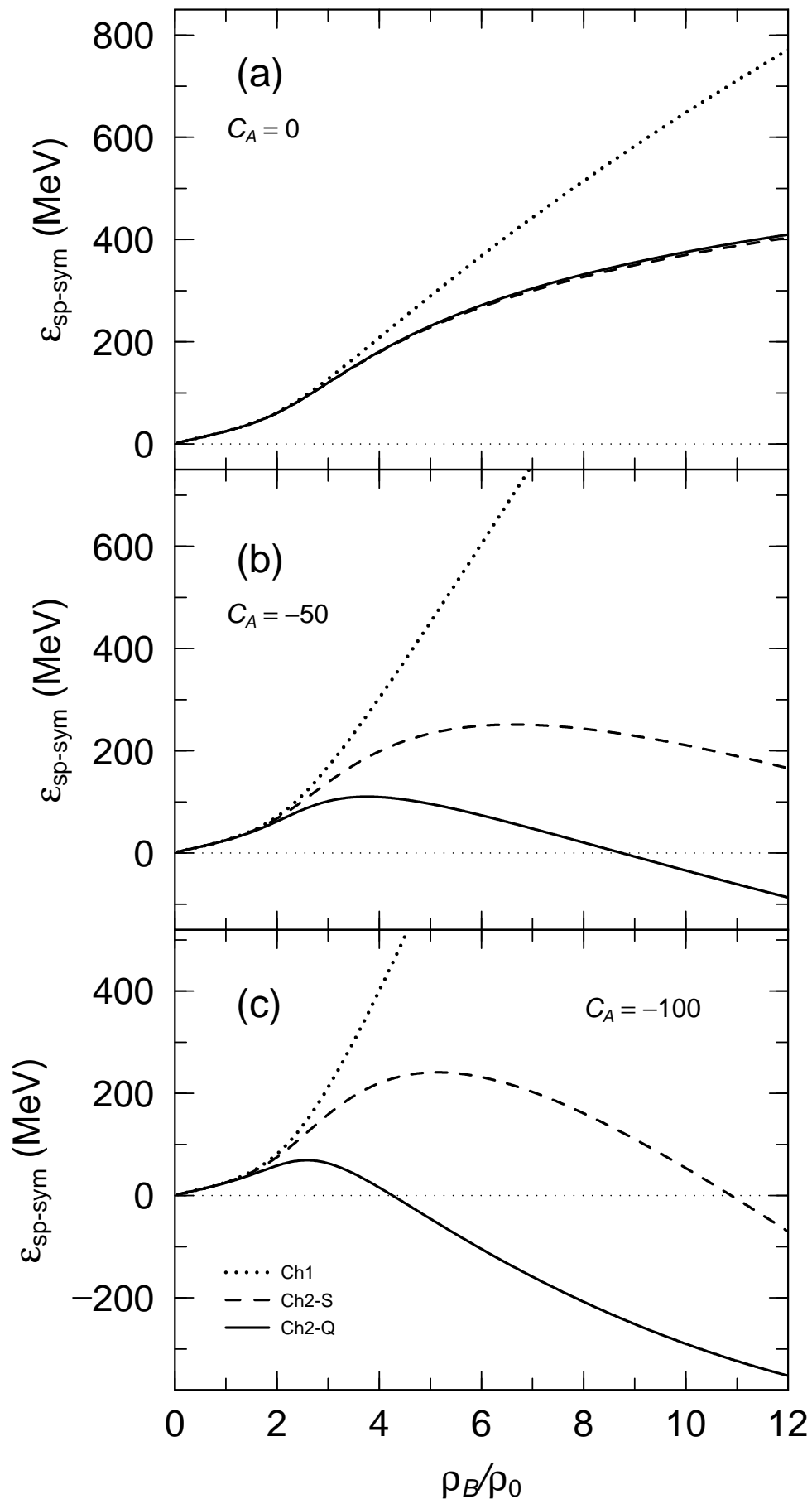


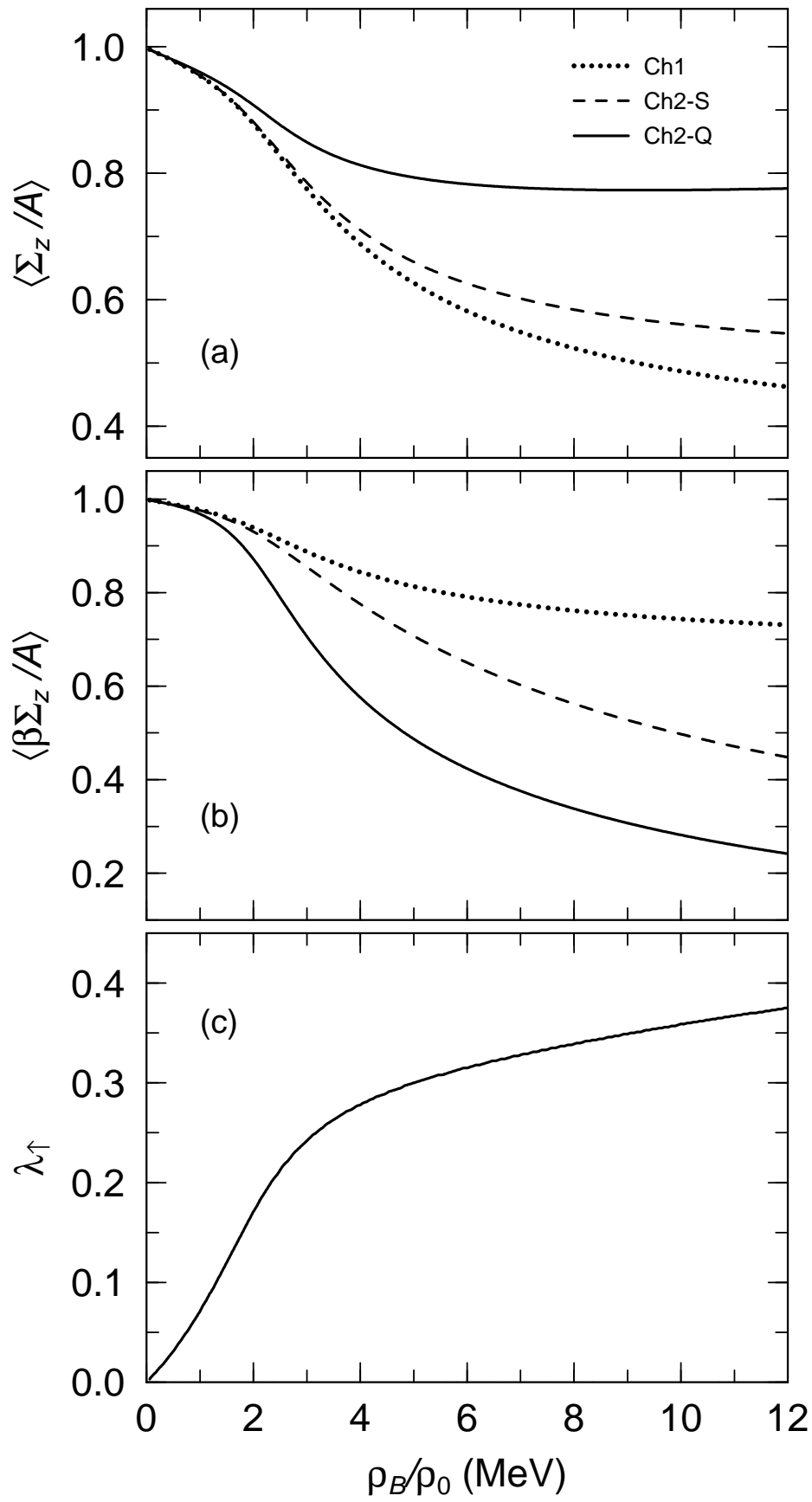


EOS FOR SPIN-ALIGNED MATTER



SPIN-SYMMETRY ENERGY





SPIN-SYMMETRY ENERGY

